Bio-electrochemical production of hydrogen and electricity from organic waste

Giorgia De Gioannis
Università degli Studi Di Cagliari: Universita degli Studi Di Cagliari
Alessandro Dell'Era
Sapienza University of Rome: Universita degli Studi di Roma La Sapienza
Aldo Muntoni
Università degli Studi Di Cagliari: Universita degli Studi Di Cagliari
Mauro Pasquali
Sapienza University of Rome: Universita degli Studi di Roma La Sapienza
Alessandra Polettini
Sapienza University of Rome: Universita degli Studi di Roma La Sapienza
Raffaella Pomi
Sapienza University of Rome: Universita degli Studi di Roma La Sapienza
Andreina Rossi
Sapienza University of Rome: Universita degli Studi di Roma La Sapienza
Tatiana Zonfa (tatiana.zonfa@uniroma1.it)
Sapienza University of Rome: Universita degli Studi di Roma La Sapienza https://orcid.org/0000-0003-3745-2767

Research Article

Keywords: cheese whey, dark fermentation, hydrogen, bio-electrochemical process

Posted Date: December 1st, 2021

DOI: https://doi.org/10.21203/rs.3.rs-1032725/v1

Abstract

This study investigated the performance of a novel integrated bio-electrochemical system for synergistic hydrogen production from a process combining a dark fermentation reactor and a galvanic cell. The operating principle of the system is based on the electrochemical conversion of protons released upon dissociation of the acid metabolites of the biological process and is mediated by the electron flow from the galvanic cell, coupling biochemical and electrochemical hydrogen production. Accordingly, the galvanic compartment also generates electricity.

Four different experimental setups were designed to provide a preliminary assessment of the integrated bio-electrochemical process and identify the optimal configuration for further tests. Subsequently, dark fermentation of cheese whey was implemented both in a stand-alone biochemical reactor and in the integrated bio-electrochemical process. The integrated system achieved a hydrogen yield in the range 75.5 – 78.8 N LH_2/kg TOC, showing a 3 times improvement over the biochemical process.

1. Introduction

Hydrogen can be used in both power generation systems and direct combustion processes, providing the great advantage of clean combustion. Moreover, H_2 is considered a very competitive energy carrier compared to other fuels, thanks to its high net heating value per unit volume. Nowadays, its use as a clean energy source is yet uncommon, while its main use is in ammonia production and hydrogenation of coal and petroleum during hydrocracking of traditional fuels (IEA 2019). However, the good environmental profile of H_2 is commonly counteracted by the fact that it is still primarily derived from non-renewable sources, with a high associated energy consumption and related relevant CO_2 emissions, posing an urgent need for sustainable production methods.

Several bioprocesses have been investigated over the last decades to produce H_2 through sustainable methods (Hallenbeck et al. 2012). Among them, dark fermentation (DF) is considered one of the most promising options. The main reason is that DF averts the major drawbacks of other biological processes (including direct or indirect photolysis and photo-fermentation), related to the intermittent production of H_2 and the need of a light source to support the process. Compared to the other biological processes, dark fermentative H_2 production has the additional advantages of higher production rate, flexibility of operation under different temperature and pressure conditions, lower net energy input and, noteworthy, applicability to a range of renewable organic sources including organic residues and carbohydrate-based wastewaters (Ghimire et al. 2015; Da Silva Veras et al. 2017; Park et al. 2021).

While DF of organic residues has been widely investigated over the past decades, the major challenges still existing for the process include the poor stability of the biochemical process and the thermodynamic/biochemical limitations to the actual H_2 production yield attainable. To this regard, when acetate is the final metabolic product of fermentation, a production of 4 moles of H_2 per mole of hexose consumed is expected, which is regarded as an upper threshold for the H_2 yield, known as the Thauer

limit (Thauer et al.1977). Therefore, of the potential 12 moles of H_2 that may be produced by one mole of glucose, only a third can be obtained biochemically. The actual H_2 yield can even be lower than the mentioned limit if other more reduced metabolic products (e.g., butyrate, ethanol) are formed or additional competing metabolic pathways occur (e.g. propionic fermentation, homoacetogenesis).

Bioelectrochemical processes (BESs) have been proposed for a variety of applications aimed at improving the performance of biological systems. Their operating principle is based on the ability of specific microorganisms defined as electroactive bacteria (EAB) to interact with solid electrodes by forming a biofilm and catalyze the oxidation of organic matter by generating an electrical potential. Microbial fuel cells (MFCs) are among the most widely investigated BESs, due to their capability of producing an electric power while simultaneously degrading an organic substrate. Generally, in the anodic chamber, where the EAB are attached to dedicated inert electrodes, the oxidation of the organic substances takes place generating CO_2 and protons, which migrate into the cathodic chamber through ion exchange membranes. The cathodic chamber is maintained under aerobic conditions, so that in the presence of electrons protons react with oxygen to produce water, resulting in the spontaneous production of electricity, the intensity and flow of which are functions of the construction features of the cell, the substrate characteristics, the inoculum and the operating conditions adopted.

A modified type of MFC, the microbial electrolysis cell (MEC), has been studied since 2005 (Liu et al. 2005b), and its scientific interest has strongly increased in recent years (Santoro et al. 2017). In that case, unlike the MFC, the cathodic chamber is maintained under anaerobic conditions; consequently, protons are reduced to H_2, since there are no others electronegative species to intercept electrons. This process requires the supply of an electric current, since the electric potential naturally generated by microorganisms is not enough to reduce H^+ to H_2. Assuming acetate as a model organic source, the electrode reactions involve oxidation to CO_2 at the anode and H^+ reduction to H_2 at the cathode (see equations 1 and 2). Assuming that the open circuit potential at the anode in an MFC is generally about $E^0 \sim -300$ mV (Liu et al. 2005b), and the minimum standard redox potential required for the cathodic reaction of $E^0 = -410$ mV (NHE) at pH 7.0, H_2 can theoretically be obtained by applying a > 110 mV circuit voltage (typically 410–300 mV to overcome internal electric resistances). However, the voltage required is significantly lower than that used for conventional water electrolysis (1.21 V at neutral pH, which can increase up to 1.8–2.0 V under alkaline conditions due to electrode overpotential), since the chemical energy extracted from organic substrates oxidized at the anode supplies most of the potential needed.

Anode: $CH_3COOH + 2H_2O \rightarrow 2CO_2 + 8e^- + 8H^+$ (1)

Cathode: $8H^+ + 8e^- \rightarrow 4H_2$ (2)

Some studies have successfully investigated BESs for exploitation of volatile fatty acids (VFAs) or DF effluents into electricity or H_2. Liu et al. (2005b) obtained 2.9 mol H_2/mol acetate applying an additional voltage of 0.250 V in a MEC. Through optimization of materials and reactor configuration, Cheng and

Logan (2007) achieved H_2 yields between 2.0 and 3.9 mol H_2/mol acetate at applied voltages of 0.2 to 0.8 V. Chae et al. (2008) showed that H_2 production gradually increases as the applied voltage is increased from 0.1 to 1 V, reaching 2.1 mol H_2/mol acetate. Liu et al. (2005a) tested power generation from acetate and butyrate in a MFC and observed that acetate is preferred over butyrate as a substrate, producing respectively 506 mW/m^2 and 305 mW/m^2.

The treatment of a real DF effluent was investigated by Chookaew et al. (2014) using both a MEC and a MFC. A power density of 92 mW/m^2 in the MFC was achieved along with 50% COD removal. When treated in the MEC, the same substrate yielded 106 mL H_2/g COD. Rivera et al. (2015) evaluated both DF effluent exploitation as a substrate for a MEC. The highest production rate (81 mL H_2/L/day) was obtained at a 550 mV voltage and was accompanied by 85% COD removal. Wang et al. (2011) performed a multi-stage process using a DF reactor for cellulose degradation followed by two MFCs that were used as power sources for a subsequent MEC. The MFCs produced a maximum of 0.43 V using the fermentation effluent that induced H_2 production in the MEC at a rate of 0.48 m^3 H_2/m^3/d and with a yield of 33.2 mmol H_2/g COD removed in the MEC. The authors observed an overall improvement in H_2 production for the integrated process by 41% compared with fermentation alone.

The integration of fermentation and electrochemical processes in the same unit has been the focus of specific studies on electro-fermentation (Moscoviz et al. 2016; Schievano et al. 2016; Yu et al. 2018). The fundamental concept is based on driving the fermentation process by modifying the redox potential through polarized electrodes placed in the reactor, which can either supply electrons or act as a sink under certain conditions. This could allow overcoming the metabolic limitations through direct electricity supply to the fermentation medium. Potential inocula include both electroactive and fermentative bacteria that can produce value-added organic acids and alcohols (Xue et al. 2018; Paiano et al. 2019), sometimes with concomitant production of H_2 and/or CH_4 (Nelabhotla and Dinamarca 2019; Toledo-Alarcón et al. 2019). Electro-fermentation is rapidly gathering attention given the successful results. To date, the study of the process is still in a preliminary stage and future developments include the orientation of the metabolic pathways towards specific end products, the selection of efficient redox mediators, the application to complex substrates and the applicability to suspended biomass configurations.

In the present work, we attempted at developing an innovative BES coupling DF with an electrochemical process, with the multiple aims of enhancing H_2 generation, exploiting the fermentation products, produce electricity and provide an internal pH buffering effect. To the best of the authors' knowledge, the concept behind the proposed process is novel and the BES developed has not been documented in other literature studies so far.

2. Materials And Methods

2.1. Integrated bio-electrochemical system; principle and setup

The integrated bio-electrochemical system (IBES) proposed here is based (see Figure 1) on the electrochemical reduction of the protons released from the dissociation of the VFAs produced during the fermentation process, leading to additional H_2 generation. The reduction reaction is mediated by the electrons released by the oxidation of a metallic element in the anodic chamber, which generates an electric current. An inert electrode, which does not take direct part in the reaction but rather plays the role of electron carrier, is placed in the fermentation medium, which is connected through an external electric circuit to the reducing electrode (anode) placed in an electrolytic solution in a dedicated chamber. The ion flow required to maintain the electroneutrality of the two electrolytes is attained through an appropriate connection between the two compartments. The reactions that occur in the cathodic (1) and anodic (2) compartments are shown below, along with the corresponding reduction potentials (E^0) in accordance with the IUPAC standard potentials convention (298 K, 1 bar, 1 M), assuming metallic Zn as the anode:

$2H^+ + 2e^- \leftrightarrow H_2$ $E^0(2H^+/H_2) = 0.000V$ (1)

$Zn \leftrightarrow Zn^{2+} + 2e^-$ $E^0(Zn_2^+/Zn) = - 0.762V$ (2)

The overall cell electromotive force under standard conditions (ΔE^0), defined as the potential difference between the cathode and the anode, for this system is as follows:

$\Delta E^0 = E^0(2H^+/H_2) - E^0(Zn^{2+}/Zn) = 0.762V$ (3)

The fact that the Gibbs free energy $\Delta G^0 = -nF\Delta E^0$ (with n = number of electrons exchanged in the reaction and F = Faraday's constant = 9.64853×10^4 C mol^{-1}) is negative (-147 kJ) ensures that the redox reaction can take place spontaneously, as the reduction potential of the anode is adequately low.

Consequently, the IBES provides, compared to the biochemical process, an additional electrochemical generation of H_2, exploiting the protons from the metabolic products. Moreover, since the system is designed as a galvanic cell, the process is energetically self-sufficient. Finally, the conversion of protons to H_2 may offer the additional benefit of contrasting the acidification of the fermentation medium, which would otherwise require the external addition of buffering agents to maintain adequate pH levels for the microbial system.

In the present work, four different experimental setups (named A, B, C, D) were designed in order to identify the most suitable materials and configuration for the IBES (Figure 2). The anode and cathode were mutually connected through an external electrical circuit equipped with a system for continuous measurement and recording of electric current and cell potential produced under load (resistor). As detailed in Table 1, the four systems differed for the compartment volume, the type of separation between the cathodic and anodic solutions (involving either a salt bridge or an anion exchange membrane, AEM) and (when applicable) the AEM surface to volume ratio (S/V). Both the salt bridge and the AEM served the purpose of allowing the ionic flow between the two compartments required to ensure the

electroneutrality of the catholyte and anolyte. The AEM was specifically selected because of its recognized acid/proton blocking capability (Xu 2005; Guo et al. 2017).

While in systems A and B the gas produced was allowed to evolve outside the system and therefore was not directly measured, systems C and D were gas-tight and also included collection, measurement and sampling of the gas generated. Dedicated H_2 leakage tests were conducted for systems C and D in order to quantify potential gas losses during the tests due to the high fugacity of H_2. The measured loss was found to lie in the range 0.12 – 0.16 mL/h for system C and 0.64 – 0.95 mL/h for system D (likely due to some minor gas leakage through the AEM), which was accounted for to quantify the amount of gas produced.

In systems A and B, the following cathode materials were selected for testing on the basis of electrical conductivity, recognized inert redox behaviour and absence of potential toxic effects on microorganisms: graphite sheet (15 cm^2), Pt sheet (2 cm^2), Ti grid (2 mm wire with mesh of 0.16 mm^2) and Ni mesh (60 mesh with 0.18 mm wire).

In all systems, the anolyte was 0.5 M Zn sulphate, while a metallic Zn plate was used as the anode.

Table 1
Summary of key features of system configurations with synthetic model solution.

	System A	System B	System C	System D
Compartment separation	Sodium chloride salt bridge	24 cm^2 AEM	11.3 cm^2 AEM	67.5 cm^2 AEM
AEM surface to volume ratio (S/V)	-	120 cm^2/L	23 cm^2/L	135 cm^2/L
Catholyte volume	0.2 L	0.2 L	0.5 L	0.5 L
Catholyte	HAc	HAc	HAc	HAc HBu
Anolyte volume	0.2 L	0.4 L	0.5 L	0.5 L
Anolyte	Zn sulphate	Zn sulphate	Zn sulphate	Zn sulphate
Cathode material	15 cm^2 Graphite sheet 2 cm^2 Pt sheet 15 cm^2 Ni mesh 15 cm^2 Ti grid	15 cm^2 Ni mesh 15 cm^2 Ti grid	10 cm^2 Ti grid	66 cm^2 Ti grid
Anode material	15 cm^2 Zn plate	15 cm^2 Zn plate	43 cm^2 Zn plate	53 cm^2 Zn plate

2.2. Materials and electrochemical/bio-electrochemical tests

In the preliminary electrochemical tests, conducted in systems A, B and C, diluted acetic (HAc) or butyric acid (HBu) was used as the model substrate to simulate the metabolic products of DF. The IBES was then tested in a batch mode using the optimized configuration D with cheese whey (CW) as the substrate; in this case, a stand-alone batch DF reactor fed with CW was employed as a reference. All tests were performed in duplicate. A summary of the experiments is reported in Table 2.

CW was collected at an Italian dairy industry producing mozzarella cheese from a mixture of cow and buffalo milk. The characteristics of CW are reported in Table 3. The samples were stored at -18°C and thawed at room temperature for approximately 24 hours before use. The pH of CW was adjusted to 7.5 using 2 M NaOH at the beginning of the DF experiments, while no further pH control was performed during the tests. The indigenous microorganisms in CW were the only active biomass source in the system. The DF tests were operated under mesophilic conditions (38 ± 1°C).

Table 2
Experimental design.

Run No.	Run code	System configuration	Cathode type	Catholyte solution
1	A-G-HAc	A	Graphite sheet	HAc
2	A-Pt-HAc	A	Pt sheet	HAc
3	A-Ti-HAc	A	Ti grid	HAc
4	A-Ni-HAc	A	Ni mesh	HAc
5	B-Ti-HAc	B	Ti grid	HAc
6	B-Ni-HAc	B	Ni mesh	HAc
7	C-Ti-HAc	C	Ti grid	HAc
8	D-Ti-HAc	D	Ti grid	HAc
9	D-Ti-HBu	D	Ti grid	HBu
10	D-Ti-CW	D	Ti grid	CW

Table 3
Characterization parameters of CW used for IBES in system D and stand-alone DF.

Parameter	Unit of measure	
Total solids	% wet weight	7.4±0.3
Volatile solids	% wet weight	6.4±0.3
Carbohydrates	g glucose-C/L	38.5±3.8
Total Organic Carbon	g C/L	39.3±3.7
pH	-	3.6±1
Acetic acid	mg HAc/L	364±71
Butyric acid	mg HBu/L	<DL
Ethanol	mg EtOH/L	3360±82
DL = detection limit		

2.3. Analytical methods

In systems C and D a volumetric gas counter with a 2 mL capacity was used for gas volume measurement, while a gas bag was employed for gas storage. In all cases the measured volume was converted under standard pressure and temperature conditions (T = 273.15 K, P = 10^5 Pa).

The biogas was periodically sampled from the gas bag with a 25 mL gastight syringe and analyzed through a gas chromatograph (Model 3600 CX, VARIAN) equipped with a thermal conductivity detector and 2 m stainless-steel packed column (ShinCarbon ST) with an inner diameter of 1 mm. The operating temperatures of the injector and detector were 100 and 130°C, respectively, with He as the carrier gas. The oven temperature was initially set at 80°C and subsequently increased to 100°C at 2°C/min.

The VFAs (acetate, butyrate, propionate, valerate, caproate, heptanoate) and ethanol concentrations were determined in 0.2-µm filtered and HCl acidified (pH = 2) liquid effluent (1 µl) with a gas chromatograph equipped with a flame ionization detector (FID) and a 30 m capillary column (TRB-WAX) with an inner diameter of 0.53 mm. The temperatures of the detector and the injector were 270 and 250°C, respectively. The oven temperature was initially set at 60°C, held for 3 min at this value, subsequently increased to 180°C at a rate of 10°C/min and finally increased to 220°C at a rate of 30°C/min and held for 2 min.

Sulphates, total and volatile solids were measured according to the Standard Methods for the Examination of Water and Wastewater (APHA AWWA and WEF 2017).

Total organic carbon (TOC) was measured using a Shimadzu TOC analyzer (TOC-VCHS and SSM-5000 module, Shimadzu, Japan).

Carbohydrates were analyzed through the colorimetric phenol–sulfuric acid method using glucose as the standard (DuBois et al. 2002).

The electrochemical process was monitored through cell voltage (ΔV) and electrical current intensity (I) measurements. The acquisition system NI cDAQ-9174 was used for this purpose and a potentiometer with a resistive load ranging from 500 Ω to 1.3 Ω was used to obtain the power curves for each system configuration. The cell voltage was measured continuously for a few minutes following each resistance variation, in order to avoid significant changes in the electrolyte solutions at the same time ensuring the achievement of equilibrium conditions. The measurement system was combined with LabVIEW as the data acquisition software.

The total amount of electric charge, Q, generated during the electrochemical process was calculated as the integral of the measured electric current, and the related theoretical amount of H_2 produced was also derived.

3. Results And Discussion

3.1. Electrochemical tests

A summary of the preliminary tests using systems A and B is provided in Table 4. The cathode characteristics were found to affect the electrochemical profile of the process, with the highest (2.2 mA) and lowest (0.77 mA) current intensities in system A being obtained with the Ti grid (run A-Ti-HAc) and graphite sheet (run A-G-HAc) electrodes, respectively. However, system A also showed the presence of a

high overpotential, likely due to the fact that salt bridges are known to generate high internal resistances (Logan et al. 2006). When the salt bridge was replaced by the AEM (system B), using a Ti cathode the cell voltage and the current intensity increased from 0.20 (run A-Ti-HAc) to 0.43 V (run B-Ti-HAc) and from 2.2 to 4.7 mA (average of the values measured during the first hour of the tests at 90 Ω as the external load), respectively.

Figure 3 depicts the power curves derived to describe the electrical characteristics of the optimized systems (runs B-Ti-HAc, C-Ti-HAc and D-Ti-HAc). The maximum power, P, observed was 5.1 mW for D-Ti-HAc (at I = 9 mA and R = 62 Ω), 2.5 mW for B-Ti-HAc (at I = 8.5 mA and R = 33.5 Ω) and 0.6 mW for C-Ti-HAc (at I = 2.1 mA and R = 110 Ω). Since the experimental conditions of the three systems were the same apart from the S/V ratio of the AEM, the results show that this parameter played a key role in determining the power efficiency of the electrochemical cell. Run D-Ti-HAc, where the geometrical configuration was arranged to maximize the S/V ratio, indeed proved to have been optimized with regard to the electrical performance.

The process evolution over time displayed a similar profile in all the investigated systems, although with different absolute values and rates of variation of the investigated parameters. In particular, as shown in Figure 4 for C-Ti-HAc and D-Ti-HAc, the catholyte pH displayed an increasing trend as a result of proton conversion into H_2, with the typical shape of an acid-base titration curve that reached a final plateau as soon as the acid dissociation was complete. The current intensity mirrored pH evolution, decreasing to almost zero as pH levelled off at the plateau. When comparing C-Ti-HAc and D-Ti-HAc, it is clear that the lower S/V ratio of the former resulted in a considerably slower current evolution and remarkably lower current intensities.

It is also worth mentioning that in all systems the electric current flow was observed to recover upon renewed addition of the proton source (data not shown), as would happen during continuous fermentation.

The anolyte pH was found to slightly increase within the first 5–6 hours of the test from an initial value of ~4.3 to a value of ~5.7, likely due to the migration of hydroxide ions from the catholyte through the AEM. The final constant pH value achieved is in good agreement with that expected in a solution in equilibrium with a $Zn(OH)_2$ precipitate ($K_s = 2 \cdot 10^{-17} - 4 \cdot 10^{-17}$). Acetate and butyrate were also clearly observed to migrate (most likely in the dissociated form, given the nature of the AEM used) to the anodic chamber over time, in compliance with electroneutrality constraints, and virtually fully transferred to this compartment at the end of the test (see the values of the percent partitioning of acetate at the anode shown in Figure 4c) for D-Ti-HAc and Figure 5b) D-Ti-HBu).

The observed trends for D-Ti-HBu (see Figure 5) of the electric current, pH of the cathodic and anodic solutions as well as the acid dissociation behaviour and migration of anionic species through the AEM were identical to run D-Ti-HAc. This prospectively indicates that the electrochemical process investigated can be applied to a fermentation system where an array of organic acids is generated.

A summary of the assessment of the process performance of C-Ti-HAc, D-Ti-HAc and C-Ti-HBu is provided in Table 5. The reported data provide a comparison between the observed cumulative H_2 production and the total theoretical H_2 yield expected based on either the overall amount of electric charge generated or the overall amount of protons derived from acid dissociation.

Taking into account the potential gas losses (see paragraph 2.1), the data in Table 5 show that the total volume of H_2 produced is consistent with the total theoretical volume of H_2 produced calculated from mobilized electrons. The released protons, assuming complete dissociation of the acid, appear to be totally reduced to H_2 ($V_{H2,th}/V_{H2,max}$) for C-Ti-HAc, albeit at a slower production rate, and for D-Ti-HAc, while for D-Ti-HBu the conversion was 90%.

Table 4
Main results for systems A and B (average values during the first hour with a fixed external resistive load of 90 Ω.

Parameters	Unit of measure	Run					
		A-G-HAc	A-Pt-HAc	A-Ti-HAc	A-Ni-HAc	B-Ti-HAc	B-Ni-HAc
Cell voltage	mV	70	80	200	100	430	350
Electric Current intensity	mA	0.77	0.93	2.20	1.07	4.68	3.70

Table 5
Summary of preliminary results concerning evolution over time in systems C and D.

	Unit of measure	C-Ti-HAc	D-Ti-HAc	D-Ti-HBu
Initial amount of acid at the cathode	mol	0.0197	0.0196	0.0134
Time to the pH/current plateau	h	645	100	74
Mobilized electrons (1)	mol e^-	0.0196	0.0174	0.0120
Total theoretical volume of electrochemical H_2 produced, $V_{H2,th}$ (2)	NL H_2	0.220	0.223	0.135
Total measured volume of H_2, $V_{H2,meas}$	NL H_2	0.127	0.092	0.053
Expected H_2 losses, $V_{H2,loss}$	NL H_2	0.077 – 0.103	0.105 – 0.156	0.064 – 0.095
Total volume of H_2 produced, $V_{H2,pr}$ (3)	NL H_2	0.205 – 0.230	0.197 – 0.249	0.117 – 0.149
Maximum theoretical volume of electrochemical H_2, $V_{H2,max}$ (4)	NL H_2	0.221	0.219	0.150
$V_{H2,pr}/V_{H2,th}$	%	93 – 105	88 – 112	87 – 111
$V_{H2,pr}/V_{H2,max}$	%	93 –104	90 – 113	78 – 99
$V_{H2,th}/V_{H2,max}$	%	99	102	90

(1) calculated from the total measured amount of electric charge

(2) calculated from mobilized electrons

(3) $V_{H2,meas} + V_{H2,loss}$

(4) Calculated from the released protons assuming complete dissociation of the acid

3.2. Bio-electrochemical tests

Figure 6a) shows the evolution of the cumulative H_2 production for the stand-alone DF reactor and the IBES, while the profiles of pH of the biological compartment and current intensity are reported in Figure 6b). The experimental data indicate a final yield of, respectively 22.4 NL H_2/kg TOC and 68.7 NL H_2/kg TOC (the latter corresponding to 75.5 – 78.8 NL H_2/kg TOC considering the H_2 leakage through the AEM), and a total duration of H_2 production of 32 and 44 h. As observed in our previous experiments on dark fermentation of various organic substrates, the biological process stopped as soon as the degradation of carbohydrates, which are the preferred substrate for H_2 generation, was complete. The generation of

organic acids as the metabolic products of fermentation was therefore virtually complete after 32 h (DF alone) and 44 h (IBES) from the start of the experiments, concomitantly with the pH plateau at 5 – 5.5.

From the data in Figure 6a) it is therefore evident that the IBES attained a significant improvement in H_2 production (by 3 times) over the stand-alone DF. In order to assess the advantages of the IBES over the conventional DF process, an attempt was made at separating the contributions of the biological and the electrochemical processes to the total H_2 yield. The green dashed curve in Figure 6a) represents the theoretical volume of H_2 that would be expected from the electrochemical reactions on the basis of the measured electric charge mobilized. If the biological and the electrochemical processes were additive, such a volume would add up to the volume generated by the biochemical process alone. According to such hypotheses, a total yield at the plateau of cumulative H_2 production of 63.4 NL H_2/kg TOC would be expected, that is 19 – 24% lower than the actual value obtained for the IBES.

It is thus tempting to hypothesize that, further to the additional volume of H_2 produced by chemical reduction of protons, the electrochemical process exerted a synergistic effect on the fermentation reactions, enhancing H_2 generation associated to the biochemical metabolic pathways. While such an effect could in principle be related to a pH buffering effect caused by the conversion of protons to H_2, this was in fact found to be relatively minor (see the pH profiles in Figure 6b). Other effects are thus claimed to have played a role during the process, including changes in the redox potential of the fermentation medium caused by the electricity flow. Concerning this, several studies on BESs, and more specifically on electro-fermentation, have demonstrated that fermentation pathways can be electrically enhanced if improved electron transport routes and energy conservation mechanisms in biomass take place. It is recognized that changes in the extracellular redox potential (ORP) may affect the intracellular redox homeostasis and metabolism of microbial cells. As a consequence, changes in fermentation metabolites (Liu et al. 2013) can occur. This concept can be advantageously exploited in anaerobic processes, because the standard ORP for the redox pair O_2/H_2O (E^0 = +820 mV) is the highest among the other pairs associated to intracellular metabolism (i.e., H^+/H E^0 = – 420 mV; NAD^+/NADH E^0 = – 320 mV; $NADP^+$/NADPH = – 315 mV). Therefore, with no O_2 in the system, electrons can be more easily accepted by intermediate metabolites. Possible ways through which electron supply may affect the fermentation process include NADH reduction and may also promote the production of additional ATP (Schievano et al. 2016). Toledo-Alarcón et al. (2019) showed that even a small amount of electrons can have a significant effect on the metabolic pathways, affecting H_2 production (with an improvement in H_2 yield by 1.8 – 2.5 times compared to conventional DF), almost irrespective of the applied potential. The authors suggested that small changes in ORP can affect the regulation of hydrogenase involved in H_2 production, due to its high sensitivity to ORP variations.

The enhancement of the fermentation reactions when coupling the biological process with an electrochemical system was also reported by Paiano et al. (2019), who observed an increased amount of metabolic products when exogenous redox mediators were used.

Table 6 shows the concentration of the metabolic products in the cathodic and anodic compartments of the IBES and the stand-alone DF reactor. These mainly included HAc, HBu and EtOH, although EtOH concentration did not differ consistently from the initial value. It can be observed that the concentrations of HBu and the total metabolic products were higher in the IBES than in the stand-alone DF. The higher amounts of metabolic products measured in the IBES are consistent with its larger observed H_2 generation compared to conventional fermentation. While clarifying the electro-stimulation of the fermentation pathways was beyond the scope of the present study, the results yet show that the integration of the biochemical and electrochemical processes produced larger than additive effects on H_2 generation.

The data in Table 6 also show that, unlike the tests using the model acid solutions, the extent of migration of the organic metabolites towards the anode was only minor. This was due to the larger complexity of the chemical composition of CW compared to the model solutions used in the previous tests, with other anionic species (presumably with smaller ionic radiuses) being likely responsible for ensuring the electroneutrality balance.

As mentioned above, the buffering effect associated to proton consumption in the IBES was mainly visible during the first stages of the process (see pH profiles in Figure 6b), but it was not capable of contrasting the progressive acidification of the cathode solution caused by the accumulation of volatile fatty acids produced during fermentation. Towards the end of the test, pH approached a value of ~3.5 for both tests, which was mirrored by a drop in the current flow. The unexpected decline in current intensity after ~45 h was probably related to a passivation effect of the anode likely caused by the precipitation of $Zn(OH)_2$ onto its surface (also evident upon visual inspection).

Table 6
Metabolic products at the end of IBES (run D-Ti-CW) and stand-alone DF.

		IBES catholyte	IBES anolyte	Stand-alone DF
Acetic acid	mg HAc/L	1188±333	454±26	1247±235
Butyric acid	mg HBu/L	3493±293	746±266	1756±110
Ethanol	mg EtOH/L	2428±192	<DL	3505±12
Total metabolites (as C)	mg $C_{VFAs+Eth}$/L	3643±73	588±155	3281±160
DL = Detection limit				

4. Conclusions

The purpose of this preliminary work was exploring the feasibility and performance of a novel IBES which is aimed at improving the H_2 yield during DF through protons reduction into H_2 mediated by a self-generated electron flow.

Preliminary tests were carried out through different configurations using a model solution to assess the electrochemical process. They highlighted the importance of optimizing the reactor design in order to reduce internal resistances and provide an appropriate H_2 generation rate along with electricity production. According to the electric current production that was measured and the flow of dissociated organic acid through the AEM, it was concluded that the model solution was almost (90 – 100%) dissociated and the protons were virtually fully converted into H_2.

The experimental tests on the bio-electrochemical integration were performed through DF of CW, without inoculum, in the optimized reactor configuration. Under this condition, IBES achieved an H_2 yield of 75.5 – 78.8 NL H_2/kgTOC that, compared to the stand-alone DF (22.4 NL H_2/kg TOC) show a 3-time improvement.

The results from the proposed IBES appear to be promising. Future aspects to investigate in further detail to derive a better understanding of the process include the potential electrochemical stimulation effects on biomass and the strategies to prevent the passivation of the anode, as such phenomena likely played a role in the experiments performed.

Declarations

Data availability statement

The authors state that the data generated during this study are mostly included in this published article in graphic form. The complete datasets generated during the current study are also available from the corresponding author on reasonable request.

References

1. APHA, AWWA (2017) WEF Standard Methods for the Examination of Water and Wastewater, 23rd Edition
2. Chae K-J, Choi M-J, Lee J et al (2008) Biohydrogen production via biocatalyzed electrolysis in acetate-fed bioelectrochemical cells and microbial community analysis. Int J Hydrogen Energy 33:5184–5192
3. Cheng S, Logan BE (2007) Sustainable and efficient biohydrogen production via electrohydrogenesis.PNAS104:. https://doi.org/10.1111/j.1365
4. Chookaew T, Prasertsan P, Ren ZJ (2014) Two-stage conversion of crude glycerol to energy using dark fermentation linked with microbial fuel cell or microbial electrolysis cell. N Biotechnol 31:179–184
5. Da Silva Veras T, Mozer TS, da Costa Rubim Messeder, dos Santos D, da Silva César A (2017) Hydrogen: Trends, production and characterization of the main process worldwide.Int. J. Hydrogen Energy

6. DuBois M, Gilles KA, Hamilton JK et al (2002) Colorimetric Method for Determination of Sugars and Related Substances. Microb Cell Fact 8:59
7. Ghimire A, Frunzo L, Pirozzi F et al (2015) A review on dark fermentative biohydrogen production from organic biomass: Process parameters and use of by-products. Appl Energy 144:73–95
8. Guo R, Wang B, Jia Y, Wang M (2017) Development of acid block anion exchange membrane by structure design and its possible application in waste acid recovery. Sep Purif Technol 186:188–196
9. Hallenbeck PC, Abo-Hashesh M, Ghosh D (2012) Strategies for improving biological hydrogen production. Bioresour. Technol
10. IEA (2019) World Energy Outlook 2019 – Analysis - IEA. https://www.iea.org/reports/world-energy-outlook-2019. Accessed 23 Mar 2020
11. Liu C-G, Xue C, Lin Y-H, Bai F-W (2013) Redox potential control and applications in microaerobic and anaerobic fermentations. Biotechnol Adv 31:257–265
12. Liu H, Cheng S, Logan BE (2005a) Production of electricity from acetate or butyrate using a single-chamber microbial fuel cell. Environ Sci Technol 39:658–662
13. Liu H, Grot S, Logan BE (2005b) Electrochemically Assisted Microbial Production of Hydrogen from Acetate. https://doi.org/10.1021/ES050244P
14. Logan B, Hamelers B, Rozendal R et al (2006) Microbial Fuel Cells: Methodology and Technology. 40:5181–5192. https://doi.org/10.1021/es0605016
15. Moscoviz R, Toledo-Alarcón J, Trably E, Bernet N (2016) Electro-Fermentation: How To Drive Fermentation Using Electrochemical Systems.Trends Biotechnol.34:856–865
16. Nelabhotla ABT, Dinamarca C (2019) Bioelectrochemical CO 2 reduction to methane: MES integration in biogas production processes. Appl Sci 9:16–18
17. Paiano P, Menini M, Zeppilli M et al (2019) Electro-fermentation and redox mediators enhance glucose conversion into butyric acid with mixed microbial cultures.Bioelectrochemistry130:. https://doi.org/10.1016/j.bioelechem.2019.107333
18. Park JH, Chandrasekhar K, Jeon BH et al (2021) State-of-the-art technologies for continuous high-rate biohydrogen production. Bioresour Technol 320:124304
19. Rivera I, Buitrón G, Bakonyi P et al (2015) Hydrogen production in a microbial electrolysis cell fed with a dark fermentation effluent. J Appl Electrochem 45:1223–1229
20. Santoro C, Arbizzani C, Erable B, Ieropoulos I (2017) Microbial fuel cells: From fundamentals to applications. A review.J Power Sources. https://doi.org/10.1016/j.jpowsour.2017.03.109
21. Schievano A, Pepé Sciarria T, Vanbroekhoven K et al (2016) Electro-Fermentation – Merging Electrochemistry with Fermentation in Industrial Applications.Trends Biotechnol.34:866–878
22. Thauer RK, Jungermann K, Decker K (1977) Energy Conservation in Chemotrophic Anaerobic Bacteria. Bacteriol Rev 41:100–180
23. Toledo-Alarcón J, Moscoviz R, Trably E, Bernet N (2019) Glucose electro-fermentation as main driver for efficient H2-producing bacteria selection in mixed cultures. Int J Hydrogen Energy 4:2230–2238

24. Wang A, Sun D, Cao G et al (2011) Integrated hydrogen production process from cellulose by combining dark fermentation, microbial fuel cells, and a microbial electrolysis cell. Bioresour Technol 102:4137–4143
25. Xu T (2005) Ion exchange membranes: State of their development and perspective. J Memb Sci 263:1–29
26. Xue G, Lai S, Li X et al (2018) Efficient bioconversion of organic wastes to high optical activity of L-lactic acid stimulated by cathode in mixed microbial consortium. Water Res 131:1–10
27. Yu Z, Leng X, Zhao S et al (2018) A review on the applications of microbial electrolysis cells in anaerobic digestion. Bioresour Technol 255:340–348

Figures

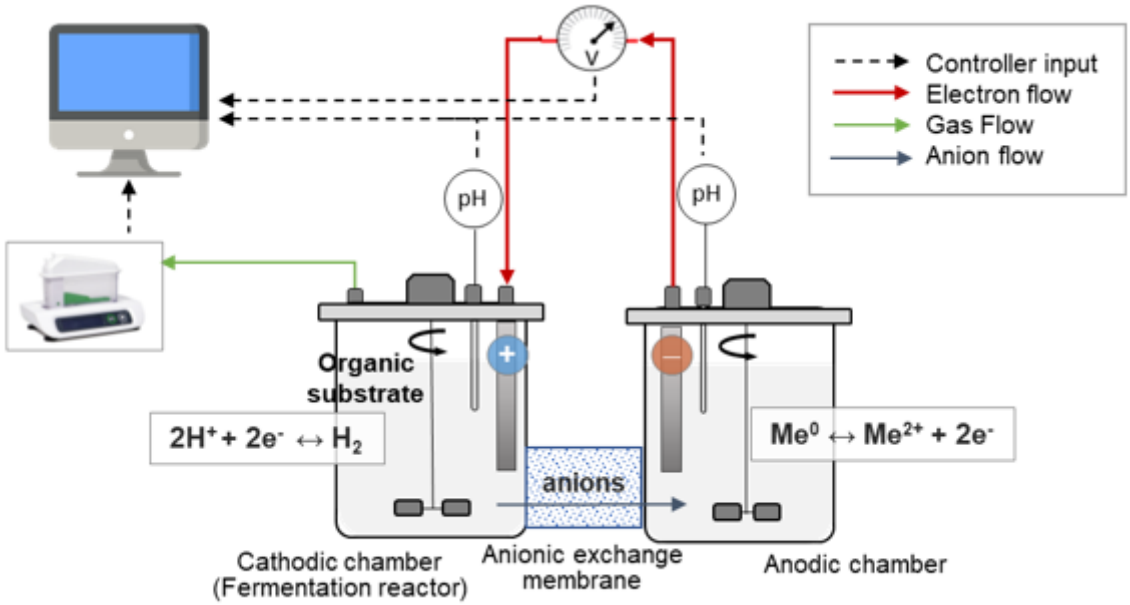

Figure 1

Layout of the IBES

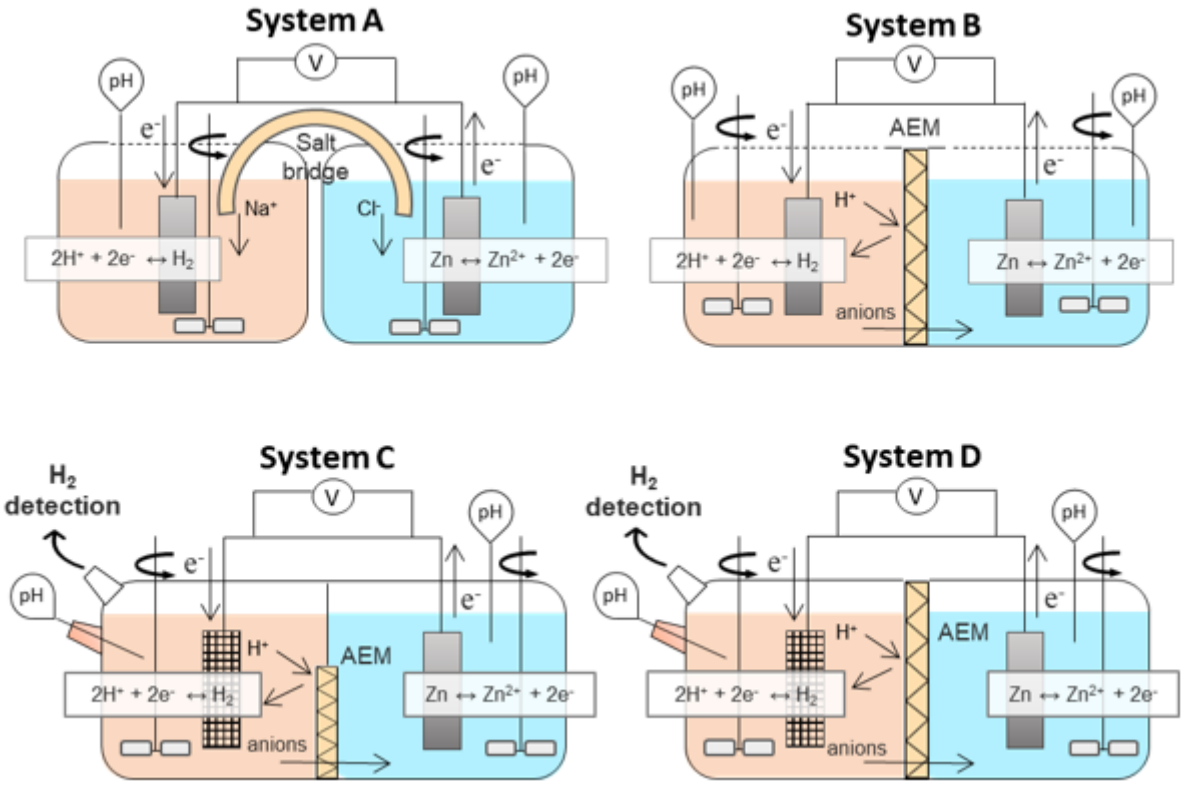

Figure 2

Schematic IBES experimental setups

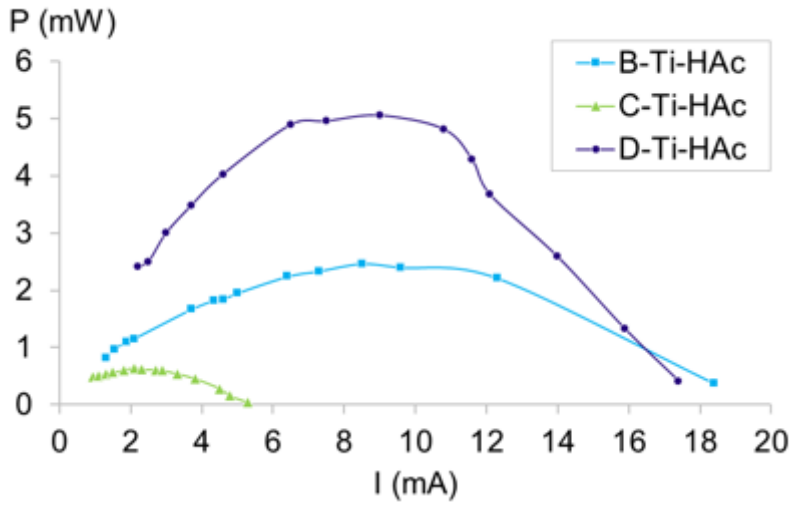

Figure 3

Power curves for B-Ti-HAc, C-Ti-HAc and D-Ti-HAc showing the influence of the S/V ratio

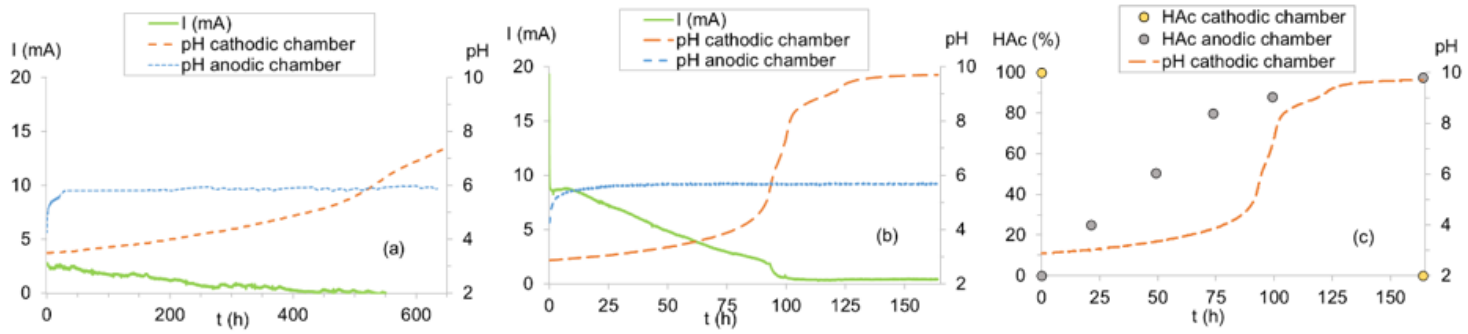

Figure 4

Time evolution of catholyte and anolyte pH and current intensity for (a) C-Ti-HAc and (b) D-Ti-HAc; (c) catholyte pH and acetate partitioning among the two chambers for D-Ti-HAc

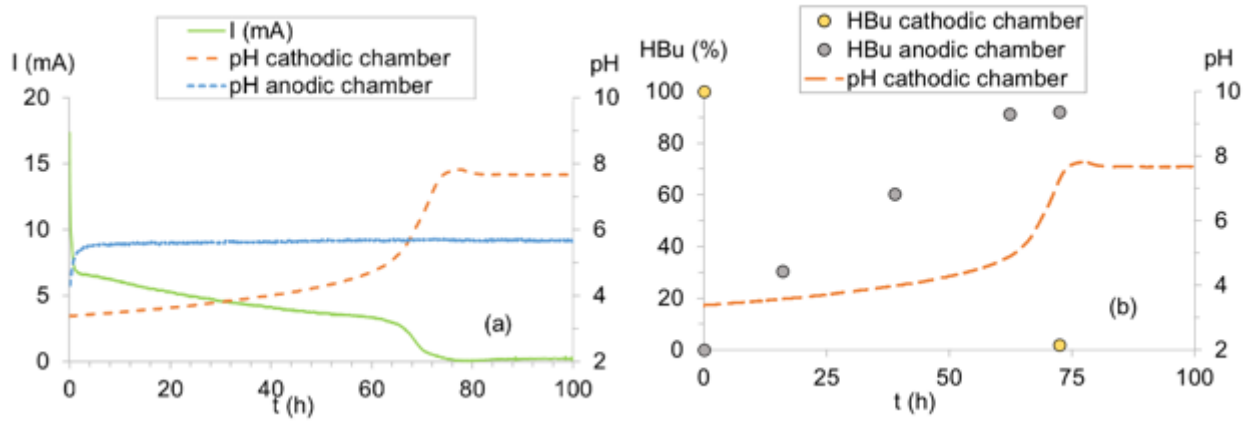

Figure 5

Time evolution of catholyte and anolyte pH and current intensity for D-Ti-HBu (a); (b) catholyte pH and butyrate partitioning among the two chambers for D-Ti-HBu

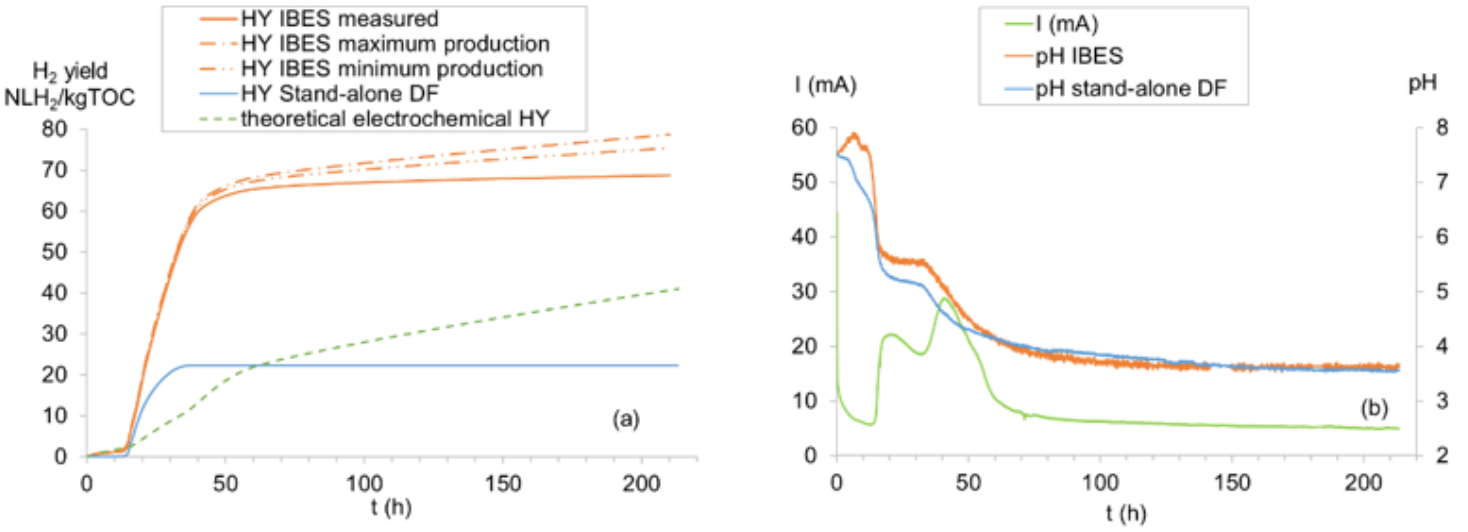

Figure 6

a) Comparison between the stand-alone DF and IBES in term of H2 yield and theoretical electrochemical H2 yield calculated from charge (green dashed line); b) pH evolution over time in both systems and electricity production in the IBES

Supplementary Files

This is a list of supplementary files associated with this preprint. Click to download.

- graphicalabstractIBES.docx